Proceedings of the Design Society, Volume 5: ICED25
https://doi.org/10.1017/pds.2025.10128

Design and mechanics of 3D printed synthetic organ tubules for biomedical applications

Michael Tomori and Paul F Egan

Texas Tech University, USA

paul.egan@ttu.edu

ABSTRACT: There is a need for design of synthetic organs due to the high demand of organ replacements for patients and low availability of alternatives. Recent advancements in additive manufacturing are enabling the creation of biomimetic organs with biocompatible materials suitable for use in the body. Here, we consider a design, build, test approach for creating synthetic blood vessel tubules by comparing fused deposition modelling and stereolithography printing processes. Tubules were printed with vessel diameters from 10 mm to 20 mm and wall thicknesses of 1 mm to 2.5 mm. Mechanical testing results demonstrated high elongation of tubules prior to breaking. Results highlight the possibility for designers to create flexible biomimetic structures to aid biomedical applications, which opens the doors for new types of patient treatments in organ repair and transplantation.

KEYWORDS: additive manufacturing, biomedical design, bio-inspired design / biomimetics, mechanics

1. Introduction

New design solutions are needed to address the shortage of available options for organ transplants and repair, which is challenging due to the multiple disciplines required to assess problems and create solutions. According to World Health Organization's (WHO), thousands of patients die each year while waiting for a suitable organ donor (Bastani, 2020; Girlanda, 2016). Despite the rapid growth of the waiting list, less than one-third of patients waiting can obtain organs that are a match from donors (Dickert-Conlin et al., 2019). Even after the transplant, patients often face the risk of organ rejection, which occurs when the immune system attacks the transplanted organ. If synthetic organs were created that were adopted and functional in the human body they could address the shortage of transplant organs available for persons and have widespread impact for human health. Here a design, build, test approach using additive manufacturing is considered for creating synthetic organs using additive manufacturing approaches (Atala et al., 2012; Egan et al., 2016; Laurence et al., 2015), which can provide customizable solutions for widespread adoption and acceptance.

Design and material selection is critical in synthetic organ fabrication and are an essential aspect of 3D printing processes that can be used to construct synthetic organs to mimic mechanical properties of elasticity, strength, and durability which are essential for functionality (Jang, 2017). Mechanical properties are essential to consider for synthetic organs to function (Liu & Wang, 2020; Wang et al., 2021) and are influenced by materials that can also affect biological adoption (Ozbolat, 2015). In the case of blood vessels it is essential to mimic the geometry of the vessel and its mechanics to ensure its flexibility to survive in the body while transporting essential fluids (Hann et al., 2022). By focusing on tubule shaped blood vessel design (Fig. 1), it is possible to develop design methods and approaches that are generalizable to further systems and health applications.

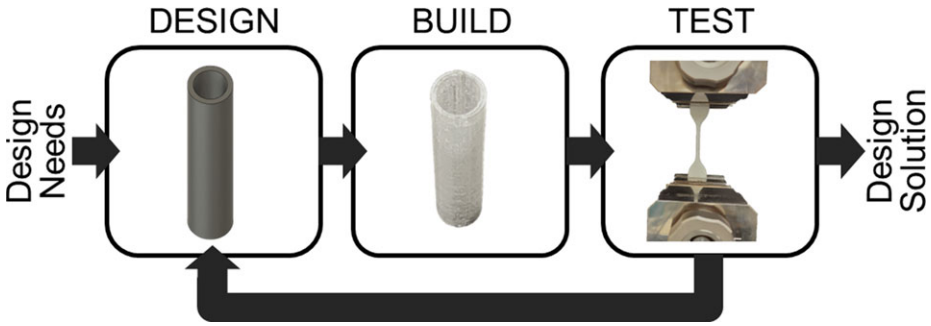

Figure 1. Design process for mechanical characterization of 3D printed organ tubules

Figure 1 consists of key steps of design, build, and testing for synthetic organ tubules fabricated using 3D printing processes. The design needs are input by considering the geometry and mechanical characteristics of the system, such as mimicking the properties of biological tissues using tubules that recreate blood vessel functionality (Xue et al., 2023; Yilmaz, 2024). The design phase relies on parameterizing the system to create different geometries that are constructed with selected materials and printing processes. The testing step is used to validate that the mechanical behavior of the system is relevant based on the designed geometry, which for biological tissues is often porous and hyper-elastic (Egan et al., 2019; Marechal et al., 2021). Once an iteration is completed, information learned can lead to a final product design or to improve solutions by altering design and build processes.

This research work's purpose is to use a design, build, test approach to assess the feasibility of two different additive manufacturing technologies for creation of synthetic organ tubules. The work begins with the design of tubules of varied diameters and thicknesses followed by manufacturing the designs with two different types of biocompatible flexible polymers. Mechanical testing is conducted to determine the properties of each polymer with fitting according to 3rd order models to model the hyper-elastic response of the materials. Finally, another design iteration is conducted to print organ tubules in a complex design shape to mimic blood vessel patterning. Novelty in the study stems from the characterization of new types of materials incorporated into designs through parametric alterations to determine feasibility. The work is impactful for designers by systematically exploring a new means of creating biomimetic systems with features that match or surpass those of the human body. The work provides a significant step forward in empirically supported design approaches for the creation and characterization of biomedical solutions. The case study of interest provides a foundation for future design approaches in medicine to address challenging shortages in organ replacement solutions for patients.

2. Methods

2.1. Design parameters

Tubule designs were created by extruding a hollow cylindrical shape to a specified height H, with outer diameter OD, and wall thickness t, as demonstrated in Figure 2 for generated CAD designs.

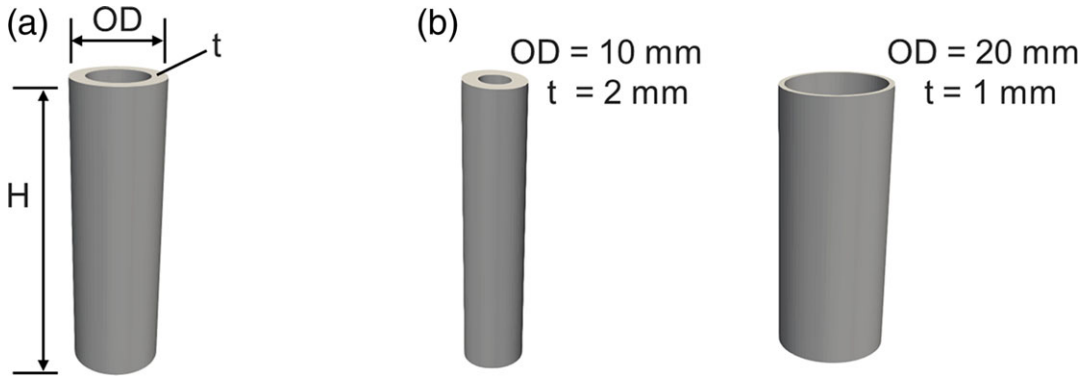

Figure 2. Design (A) Parameters for tubules with (B) Example designed prints

The wall thickness adds material from the outer diameter dimension towards the inside of the tubule, thereby the tubules have an inner diameter ID dependent on the specified wall thickness that dictates the void volume within the tubule for fluid flow. Six different designs for tubules were created that had varied combinations of outer diameter and thickness values. Outer diameters included 10 mm, 15 mm, and 20 mm paired with wall thicknesses of 1 mm or 2.5 mm. Figure 2B highlights the two extreme designs generated: One design has the largest thickness with lowest outer diameter possible and the other design with the largest outer diameter and lowest thickness possible. Height for all designs was set to 50 mm.

2.2. Fused deposition modelling

Two samples of each design were first fabricated using fused deposition modeling printing (FDM) with thermoplastic polyurethane (TPU) material. The process involved extruding molten TPU filament through a nozzle and depositing it layer by layer to form complex geometries (Fig. 3). The Anycubic Kobra 3D printer was used to fabricate designs. The fabrication process began by creating a digital version of the design using CAD software, then exporting it as an STL file, and slicing using Ultimaker Cura software. All parts were printed in the vertical orientation and required no support material.

Figure 3. Extrusion printer with highlighted part

Printing parameters included the nozzle temperature at 210°C (to melt the TPU) and bed temperature at 60°C. Before printing, the print bed was cleaned and properly levelled to ensure optimal adhesion. Once the printer started, the TPU filament was fed into the nozzle, where it was melted and extruded onto the print bed to build the tubule.

2.3. Stereolithography

Two samples of each design were then created using stereolithography (SLA) technology with BioMed Elastic 50A resin (Formlabs) as demonstrated in Figure 3. SLA is a higher resolution 3D printing process than FDM that uses a laser to cure liquid resin layer by layer to form parts. All parts had support material added and were printed in the horizontal orientation.

To operate the printer, the Elastic 50A resin was loaded into the resin tank of the SLA printer, then the build platform was prepared and mounted. The SLA printer began by directing a laser across the resin's surface, following the cross-sectional pattern of the first layer. The laser solidified the resin where it was traced, creating the first layer of the print. Afterward, the build platform moved up, a new layer of liquid resin was deposited, and the laser cured layers sequentially to form a complete design. Once the printing process was complete, the build platform was raised, and the fully printed specimen was removed from the platform. To eliminate any residual uncured resin, the part was washed in isopropyl alcohol, ensuring the surface was clean and free from excess material. The washed sample was then placed into a Form Cure station for post-curing. During post-curing, the sample was exposed to ultraviolet (UV) light and heated to 60°C for 20 minutes to fully cure the resin. After printing support material was removed manually with a precision cutting tool.

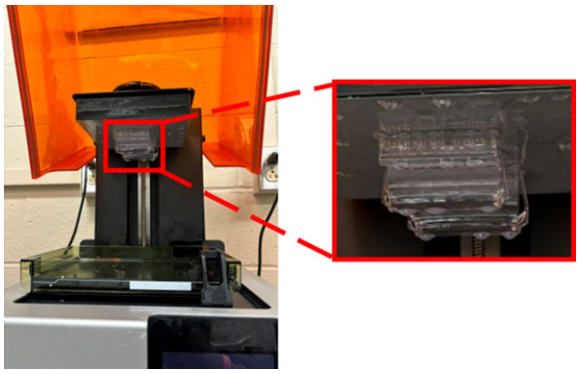

Figure 4. Stereolithography printer with highlighted part

2.4. Mechanical characterization

Mechanical characterization was carried out by creating tensile bar specimens to measure the mechanical properties of the printed materials. Tensile bar specimens were created according to the ASTM D412 standards, specifically as a type C dumbbell shape. Figure 4A demonstrates the printed tensile bar specimens for TPU and resin materials. Figure 4B demonstrates the samples in the tensile testing machine. Four samples were printed for each material, with each sample having a thickness of 3.4 mm, a width of 6 mm, a gauge length of 33 mm, and a total length of 115 mm. Load-displacement data was collected to calculate the true strain and true stress.

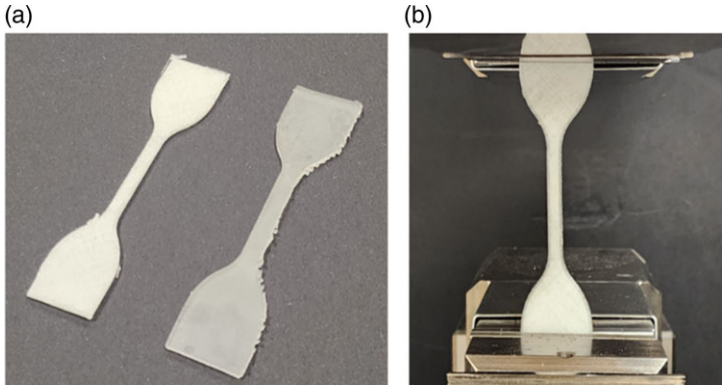

Figure 5. Mechanical testing (A) Specimens and (B) Tensile test setup

Mechanical testing was conducted with an Instron 5966 universal testing machine with pneumatic grips to prevent slippage of samples. Testing was conducted at a constant loading rate of based on displacement of 300 mm/s.

Due to the nonlinear material response of samples, hyper-elastic modelling fitting was used for analysis. The stress-strain curves were fitted to Yeoh/Ogden models to describe the material's behaviour mathematically (Garg, 2023; Ogden, 1972; Yeoh & Fleming, 1997). This modelling enables accurate predictions for mechanical responses in design applications informed by empirical measurements. CurveFitter software (WelSimulation LLC, v2.8.8760) was used to analyse the data by finding empirical constants for the Yeoh 3rd order and Oden 3rd order models considered for fitting. The Yeoh 3rd order model

$$W = \sum_{i=1}^{N} C_{i0}(\bar{I}_1 - 3) \tag{1}$$

considers true strain as the independent variable and true stress as the dependent variable with fitted values for material constants: C10, C2O, C30, I as the first invariant of the deformation tensor, and N denotes the order of the series to calculate the strain energy density W. The Ogden 3rd order model

$$W = \sum_{i=1}^{N} \frac{\mu_i}{\alpha_i}(\bar{\lambda}_1^{\alpha_i} + \bar{\lambda}_2^{\alpha_i} + \bar{\lambda}_3^{\alpha_i} - 3) \tag{2}$$

considers true strain as the independent variable and true stress as the dependent variable with fitted values for empirically informed constants μ and α according to empirical principle stretches λ with N denoting the order of the series. By fitting these models it is possible to quantify the stress-strain behaviour of each material to inform the design of tubules.

3. Results and discussion

3.1. Tubule fabrication

Two samples of each of the six tubule designs were printed using TPU and resin materials. All fabrications qualitatively printed with an unobstructed tubule shape as demonstrated for highlighted designs in Figure 6.

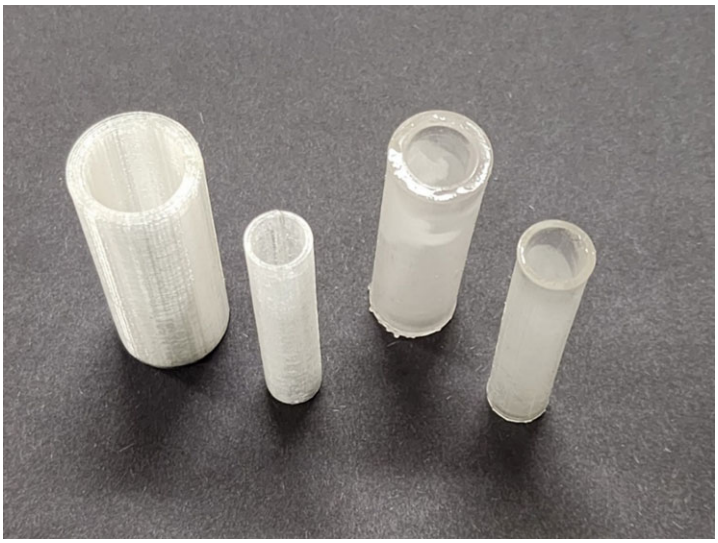

Figure 6. Fabricated tubules for TPU (left) and SLA parts (right)

Highlighted tubule fabrications in Figure 6 include for TPU a design with a 20 mm outer diameter with 2.5 mm thickness and a design with 10 mm outer diameter and 1 mm thickness. SLA designs in Figure 6 include a 15 mm outer diameter design with 2.5 mm thickness and a 10 mm outer diameter design with 1 mm thickness. To determine the dimensional accuracy of fabricated designs, all samples were measured for their thickness in four different evenly spaced locations around their diameter using veneer calipers. Results for each of the six designs for both materials are provided in Table 1 with the mean measurements (tAVG), standard deviation (tSTD), and standard error of the mean (tSEM) reported along with the originally designed dimensions for each tubule.

Table 1. Design parameters and dimensional measurements of printed tubules

Design parameters and measurements for printed tubules							
Designed Tubules					**Measured Tubules**		
Sample Number [#]	Material Printed	Outer Diameters OD [mm]	Inner Diameters ID [mm]	Wall thickness t [mm]	Mean wall thickness tAVG [mm]	Standard deviation wall thickness tSTD [mm]	Standard error of mean wall thickness tSEM [mm]
1	TPU	20	18	1.0	1.01	0.066	0.023
2	TPU	20	5	2.5	2.26	0.102	0.036
3	TPU	15	13	1.0	0.95	0.041	0.014
4	TPU	15	10	2.5	2.31	0.084	0.029
5	TPU	10	8	1.0	1.04	0.029	0.010
6	TPU	10	5	2.5	2.22	0.067	0.024
7	Resin	20	18	1.0	1.08	0.033	0.011
8	Resin	20	5	2.5	2.56	0.031	0.011
9	Resin	15	13	1.0	1.09	0.048	0.017
10	Resin	15	10	2.5	2.50	0.046	0.016
11	Resin	10	8	1.0	1.13	0.053	0.019
12	Resin	10	5	2.5	2.51	0.059	0.021

Overall, all designs printed within about 0.25 mm of their intended thickness dimensions, with a bias towards printing too large with low variation for designs according to standard error measurements. TPU samples had a consistently lower wall thickness for 2.5 mm thickness by about 0.2 to 0.3 mm but were within 0.05 mm of thickness values for 1 mm thickness designs. Resin samples showed better consistency and accuracy for printed dimensions with being at most about 0.15 mm larger than the intended design and rarely too small. These results demonstrate that both materials are suitable for recreating tubule shapes at these dimensions, with resin having a better overall consistency and accuracy.

3.2. Mechanical characterization

Figure 7 provides the mechanical testing results for the true strain and true stress response for the TPU and resin materials. Each test consists of four different printed samples of the tensile bar design to demonstrate repeatability of the measurements. Both types of material follow a non-linear hyper-elastic stress-strain material response.

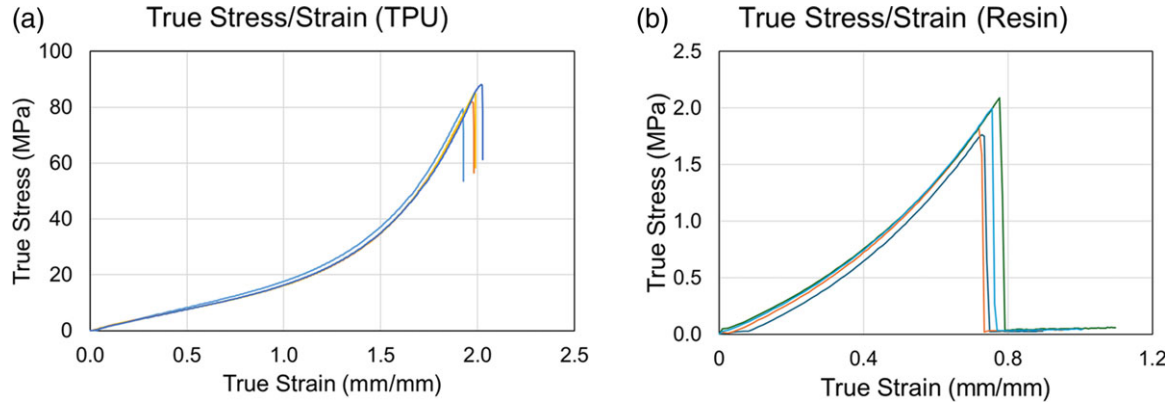

Figure 7. True stress-strain curve for (A) TPU and (B) Resin materials. Each set of data contains testing of four samples

The TPU material has a maximum extension of about 2.0 mm.mm while the resin material extends about 0.8 mm/mm prior to breaking. This demonstrates the excellent stretchability of both materials, with TPU having about twice the extensibility of the resin material. The TPU material also had a much higher peak stress of about 80 MPa compared to the peak stress of 2 MPa for the resin material. Resin samples reach their maximum stress at approximately 0.76 to 0.79 mm/mm, whereas TPU samples reach their peak at around 1.9 to 2.1 mm/mm. When considering human blood vessels as a case study, the real human body experiences a range of stress and strain values, with circumferential stress in the aorta reaching around 100-200 kPa and strain typically between 10-30% under normal physiological conditions (Plonek et al., 2017). Thereby both types of materials if implanted in the body would retain strength for physiological conditions. All samples for each material exhibit similar stress-strain responses that highlights the consistency created through the additive manufacturing processes. In Figure 8 one representative testing sample from each material is fit to 3rd order hyper-elastic models (Equations 1 and 2) to create quantitative predictions of material behaviour for designers.

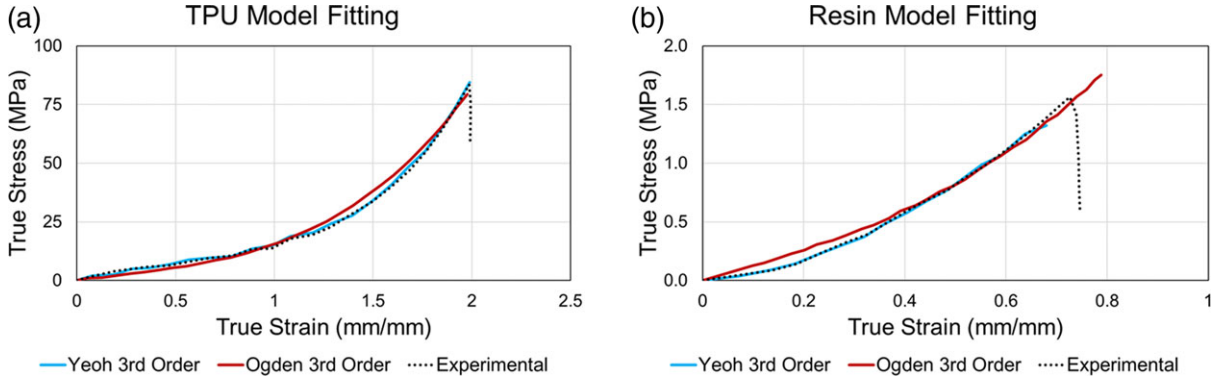

Figure 8. True stress-strain curve for (A) TPU and (B) Resin materials. Each set of data contains one set of experimental setting data fitted to 3rd order hyper-elastic models

Figure 8 demonstrates that both the Yeoh 3rd order and Ogden 3rd order models closely follow the experimental data. Both models only consider the stress-strain curves up until the point of failure. Table 2 provides quantifications of the material fitting parameters for each material and model.

Table 2. Material fitting parameters for 3rd order hyper-elastic models

Material	Fitting parameters for hyper-elastic models Yeoh 3 Order	Ogden 3 Order
TPU	C10 = 3.82316 C20 = -0.10974 C30 = 0.0945467 R2 = 0.994018	Mu1 = 0.0621817 Mu2 = 0.595262 Mu3 = -3.2591 a1 = 1.19827 × 10-6 a2 = 5.45173 a3 = -1.55676 R2 = 0.988872
Resin	C10 = 0.107646 C20 = 0.401139 C30 = -116227 R2 = 0.951617	Mu1 = 0.0226904 Mu2 = 0.158423 Mu3 = -1.06718 × 10-9 a1 = 4.51385 a2 = 5.3611 a3 = -5.29068 R2 = 0.938309

Table 2 provides parameters for equations 1 and 2 to describe the 3rd order mechanical relationship between true stress and true strain for each material. These models can be used to tune the mechanics of structures for design applications based on a specific loading condition expected in the body by adjusting tubule dimensions appropriately according to desired elongation. The high coefficient of determination for both models suggest either could reasonably be used for design applications to provide an accurate prediction of material behaviours for different conditions. Additionally, the high coefficients of determinations confirm the materials do behave according to a 3rd order response that demonstrates their hyper-elastic behaviour that can better match the expected behaviour of biomechanical components of the body in comparison to conventional linear-elastic materials.

3.3. Branching organ design

A second design iteration was conducted to form synthetic organ models from tubule shapes that are presented in Figure 9 for a branching blood vessel model. The blood vessel model was created to replicate the shape and geometry of blood vessels in the body with open channels to allow fluid flow.

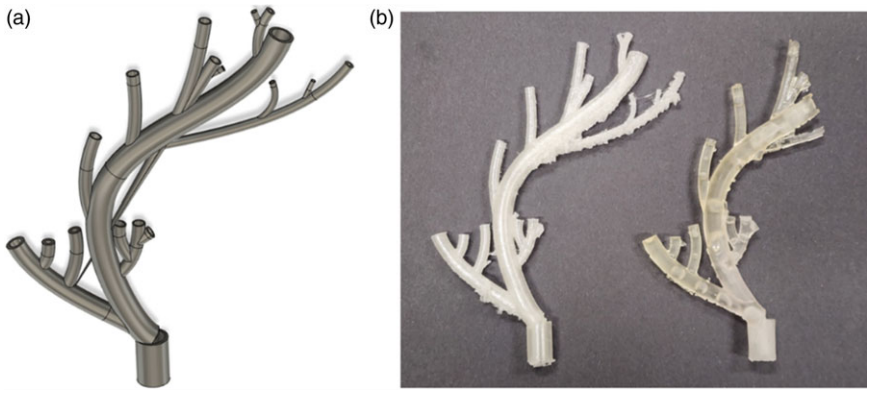

Figure 9. Branching blood vessels (A) CAD design and (B) TPU and resin prints

Figure 9A shows the CAD design model which has the base, stem, and branches and was generated with the same design parameters as tubules in Figure 2 dictating the outer diameter and wall thickness of each branch. The outer diameters were varied from 10 mm at the widest parts and 4 mm at the thinnest parts. The wall thickness was varied from 2 mm at the widest parts to 1 mm at the thinnest parts. Branches were generated to extend from the main vessel, thereby representing smaller capillaries or arterial branches to facilitate the flow of fluid with dimensions relevant to human anatomy.

Figure 9B demonstrates the branching blood vessels printed using the TPU and resin materials. Both designs printed qualitatively as expected when compared to the CAD, but there was some obstruction in the flow channel pathway, especially for the resin print where excess resin was cured within the channels. Future work can improve the prints by optimizing the print direction and support material placement to ensure more consistent formation of vessel cavities. Both printed designs retain flexibility and have outer diameter and wall thickness measurements within a similar level of error as tubule dimensions reported in Table 1. Overall, these results demonstrate the feasibility in using FDM and SLA processes to recreate blood vessel geometry for biocompatible parts with flexible mechanical behaviours that mimic physiological functionality.

Given that human blood vessels experience a normal blood pressure of approximately 120/80 mmHg, the printed design demonstrates sufficient strength and elasticity to withstand and exceed this physiological pressure based on mechanical testing. The elastic modulus and yield strength of the printed material surpass those of natural blood vessels, ensuring structural stability in expected operating conditions (Kshirsagar et al., 2006). These conditions demonstrate promise for creating high-strength biomimetic structures used with the human body that could be further advanced through additional considerations of biological and clinical testing.

3.4. Limitations and future work

The research demonstrated the feasibility of creating synthetic blood vessels with biocompatibility for potential use as organ replacements and repair through a design, build, test approach. A key goal of the work was determining the printable dimensions and accuracy of tubule prints that are limited by the physics of 3D printing technologies. FDM technology is limited by the need to flow melted polymer through a nozzle, thereby its resolution is dictated by nozzle size and fluid physics. SLA technology is limited by laser spot size and behaviour of cross-linking polymers, which is dictated by the laser specifications and material physics. Within these limitations tubules were successfully printed with features from 1 mm to 20 mm, with minor variation generally within 0.25 mm for both materials that provides a high degree of accuracy for the biomedical application. Another key limitation of the materials is how they react to the human body if used as implants, although the chosen materials are known for their biocompatibility future work is necessary to ensure they are safe for implantation in the human body. However, the design approach used for characterizing the materials would be applicable for further materials considered if alterations are necessary for biosafety.

Future work should focus on assessing actual use of materials as implants in the human body through in vitro and in vivo testing followed by clinical trials prior to widespread use. The biological testing could also consider use of design methods to create synthetic organs for applications beyond blood vessels. For instance, the creation of synthetic tissues that imitate the natural extracellular matrix and facilitate cell growth and differentiation is a potential area of study (Bhattacharya et al., 2023). Further mechanical testing for compression, bending, and other loading conditions could also help to fully characterize suitable materials for organ replacement applications. There is also great potential in using design methods to create new efficient patterns of blood vessels through computational design generation, grammars, or using imaging techniques on the body to more accurately recreate intended geometries (Yeh et al., 2020). These new approaches open doors to many design opportunities for using additive manufacturing for biomedical applications, especially where automated design processes and fabrication can lead to innovative patient-specific solutions (Akilbekova & Mektepbayeva, 2017). By adopting patient-specific approaches it is possible to use design methods to tailor solutions for each person's unique clinical needs and physiologies, which can benefit from 3D printing processes to create customized solutions on-demand in the hospital. By using 3D printing processes and materials that are widely customizable and rigorously validated for clinical use, it is possible to address organ shortages by fabricating new organs with high performance and acceptability.

The branching blood vessel model could be further refined by incorporating Murray's Law, ensuring that the printed biomaterials allow optimal flow distribution and recreate the natural geometry of branching

blood vessels (Taylor et al., 2024). Computational modeling can further refine branch diameters to match real human hemodynamics, improving blood flow efficiency (Randles et al., 2017). Also, studies should integrate computational fluid dynamics simulations to assess flow velocity profiles to determine if shear stress remains within physiological ranges and pressure drop consistency compared to physiological blood vessels. By further analyzing the mechanics of the blood vessel and resulting flow with different design configurations it is possible to better recreate the properties of natural blood vessels while also incorporating improvements that surpass natural systems.

4. Conclusions

A design, build, test approach was used to consider the creation of synthetic tubules for organ replacement using an FDM and SLA 3D printing process with TPU and Elastic 50A rein materials. Both processes were able to create tubules with diameters from 10 mm to 20 mm in width and wall thicknesses of 1 mm or 2.5 mm within about 0.25 mm of the intended dimensions which demonstrates a high degree of accuracy. The resin material had a slightly better accuracy and consistency of printing. For mechanical testing the TPU material demonstrated a higher elongation and stiffness than the resin material. A final iteration of the design demonstrated the potential for using both materials to recreate the patterning of blood vessels found in the body making it viable alternative for biomedical applications. The increased stiffness, higher strength, and thicker wall composition further contribute to its strength and expected longevity, allowing it to withstand the mechanical stress experienced by natural blood vessels. Mechanical testing results were also fit with 3rd order models that allow for prediction of material properties when redesigning tubules for specific clinical scenarios. Overall, the research demonstrates a proof-of-concept for using 3D printed materials for synthetic organs, which opens new doors for designers to work with clinicians to create personalized solutions for diverse patient needs.

References

Akilbekova, D., & Mektepbayeva, D. (2017). Patient specific in situ 3D printing. In *3D Printing in Medicine* (pp. 91–113). Elsevier.

Atala, A., Kasper, F. K., & Mikos, A. G. (2012). Engineering complex tissues. *Science translational medicine*, 4 (160), 160rv112–160rv112.

Bastani, B. (2020). The present and future of transplant organ shortage: some potential remedies. *Journal of nephrology*, 33 (2), 277–288.

Bhattacharya, A., Alam, K., Roy, N. S., Kaur, K., Kaity, S., Ravichandiran, V., & Roy, S. (2023). Exploring the interaction between extracellular matrix components in a 3D organoid disease model to replicate the pathophysiology of breast cancer. *J Exp Clin Cancer Res*, 42(1), 343. https://doi.org/10.1186/s13046-023-02926-4

Dickert-Conlin, S., Elder, T., & Teltser, K. (2019). Allocating scarce organs: How a change in supply affects transplant waiting lists and transplant recipients. *American Economic Journal: Applied Economics*, 11 (4), 210–239.

Egan, P., Cagan, J., Schunn, C., Chiu, F., Moore, J., & LeDuc, P. (2016). The D3 Methodology: Bridging Science and Design for Bio-Based Product Development. *Journal of Mechanical Design*, 138(8).

Egan, P. F., Bauer, I., Shea, K., & Ferguson, S. J. (2019). Mechanics of Three-Dimensional Printed Lattices for Biomedical Devices. *Journal of Mechanical Design*, 141(3), 031703.

Garg, H. (2023). Mechanical testing of synthetic biomaterials for organ simulation Girlanda, R. (2016). *Deceased organ donation for transplantation: challenges and opportunities*. World journal of transplantation, 6(3), 451.

Hann, S. Y., Cui, H., Chen, G., Boehm, M., Esworthy, T., & Zhang, L. G. (2022). 3D printed biomimetic flexible blood vessels with iPS cell-laden hierarchical multilayers. *Biomedical Engineering Advances*, 4, 100065.

Jang, J. (2017). 3D bioprinting and in vitro cardiovascular tissue modeling. *Bioengineering*, 4(3), 71.

Kshirsagar, A. V., Carpenter, M., Bang, H., Wyatt, S. B., & Colindres, R. E. (2006). Blood pressure usually considered normal is associated with an elevated risk of cardiovascular disease. *The American journal of medicine*, 119 (2), 133–141.

Laurence, J., Baptista, P., & Atala, A. (2015). Translating regenerative medicine to the clinic. Academic Press.

Liu, F., & Wang, X. (2020). Synthetic polymers for organ 3D printing. *Polymers*, 12(8), 1765.

Marechal, L., Balland, P., Lindenroth, L., Petrou, F., Kontovounisios, C., & Bello, F. (2021). Toward a common framework and database of materials for soft robotics. *Soft robotics*, 8 (3), 284–297.

Ogden, R. W. (1972). Large deformation isotropic elasticity–on the correlation of theory and experiment for incompressible rubberlike solids. *Proceedings of the Royal Society of London. A. Mathematical and Physical Sciences*, 326 (1567), 565–584.

Ozbolat, I. T. (2015). Bioprinting scale-up tissue and organ constructs for transplantation. *Trends in biotechnology*, 33 (7), 395–400.

Plonek, T., Zak, M., Burzynska, K., Rylski, B., Gozdzik, A., Kustrzycki, W., Beyersdorf, F., Jasinski, M., & Filipiak, J. (2017). The combined impact of mechanical factors on the wall stress of the human ascending aorta–a finite elements study. *BMC cardiovascular disorders*, 17, 1–7.

Randles, A., Frakes, D. H., & Leopold, J. A. (2017). Computational fluid dynamics and additive manufacturing to diagnose and treat cardiovascular disease. *Trends in biotechnology*, 35 (11), 1049–1061.

Taylor, D. J., Saxton, H., Halliday, I., Newman, T., Hose, D., Kassab, G. S., Gunn, J. P., & Morris, P. D. (2024). Systematic review and meta-analysis of Murray's law in the coronary arterial circulation. *American Journal of Physiology-Heart and Circulatory Physiology*, 327 (1), H182–H190.

Wang, Y., Li, X., Chen, Y., & Zhang, C. (2021). Strain rate dependent mechanical properties of 3D printed polymer materials using the DLP technique. *Additive Manufacturing*, 47, 102368.

Xue, Y.-Q., Zhang, Y.-C., Zhang, Y.-B., & Wang, J.-Y. (2023). Zein-based 3D tubular constructs with tunable porosity for 3D cell culture and drug delivery. *Biomedical Engineering Advances*, 5, 100059.

Yeh, R. Y., Nischal, K. K., LeDuc, P., & Cagan, J. (2020). Written in blood: Applying shape grammars to retinal vasculatures. *Translational Vision Science & Technology*, 9 (9), 36–36.

Yeoh, O. H., & Fleming, P. (1997). A new attempt to reconcile the statistical and phenomenological theories of rubber elasticity. *Journal of Polymer Science Part B: Polymer Physics*, 35 (12), 1919–1931.

Yilmaz, G. (2024). Foundational Engineering of Artificial Blood Vessels' Biomechanics: The Impact of Wavy Geometric Designs. *Biomimetics*, 9(9), 546.